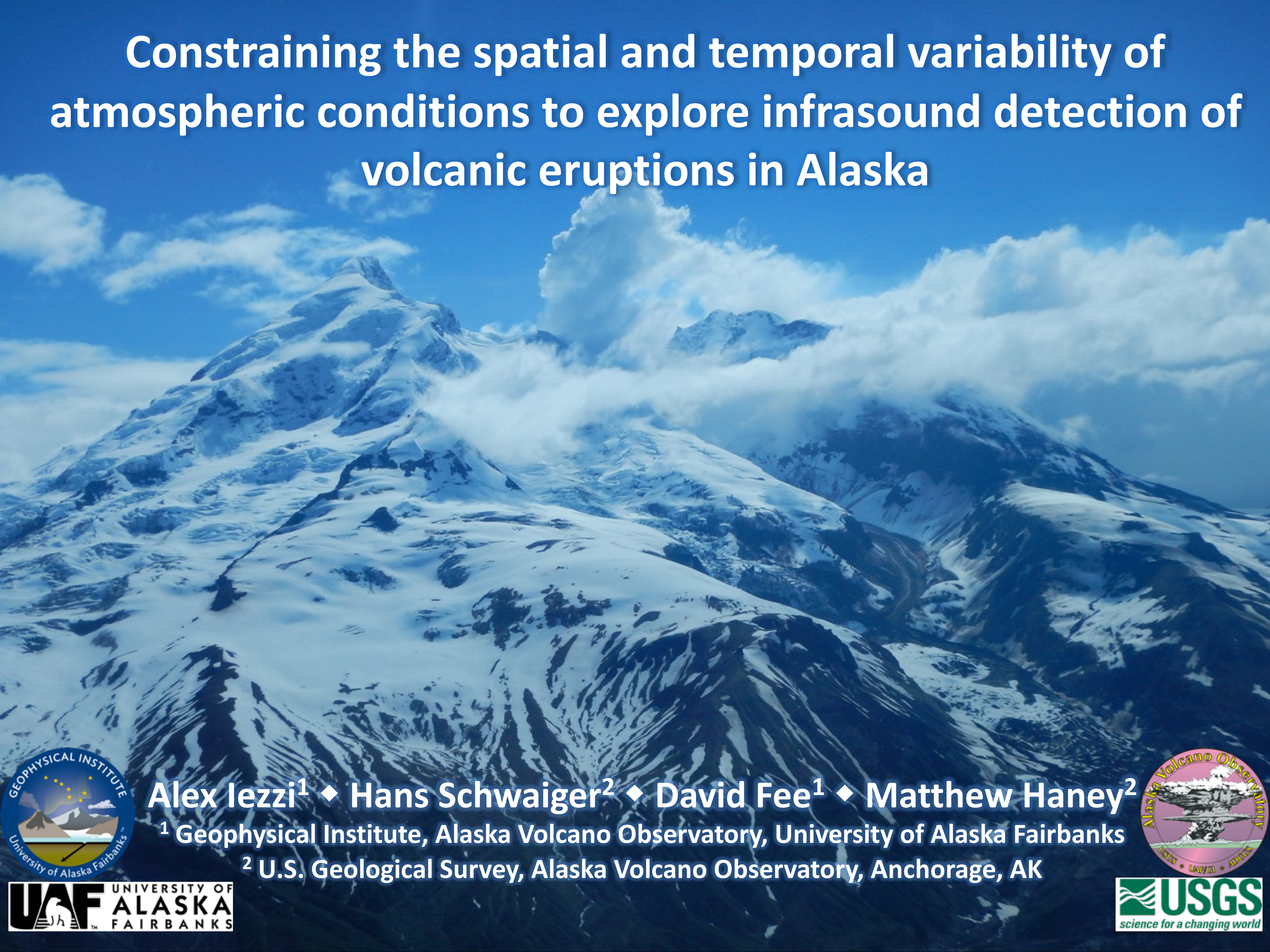

Constraining the spatial and temporal variability of atmospheric conditions to explore infrasound detection of volcanic eruptions in Alaska

Alex Iezzi[1] ◆ Hans Schwaiger[2] ◆ David Fee[1] ◆ Matthew Haney[2]

[1] Geophysical Institute, Alaska Volcano Observatory, University of Alaska Fairbanks

[2] U.S. Geological Survey, Alaska Volcano Observatory, Anchorage, AK

Motivation

- Numerous volcanic eruptions occur each year in Alaska, often in remote places with limited local monitoring
  ➡ Remote infrasound monitoring is heavily relied upon

- Long-range infrasound signals are highly influenced by the propagation path

- Atmospheric conditions (winds and temperature) can change rapidly and over short distances

- EarthScope TA enhances the infrasound monitoring network in Alaska

This Talk:

- Constrain spatio-temporal atmospheric variability
  - Velocity model of the atmosphere
  - Aid in long-range infrasound signal interpretation
- Case Studies: Distinguish between source and propagation effects of volcanic eruption signals

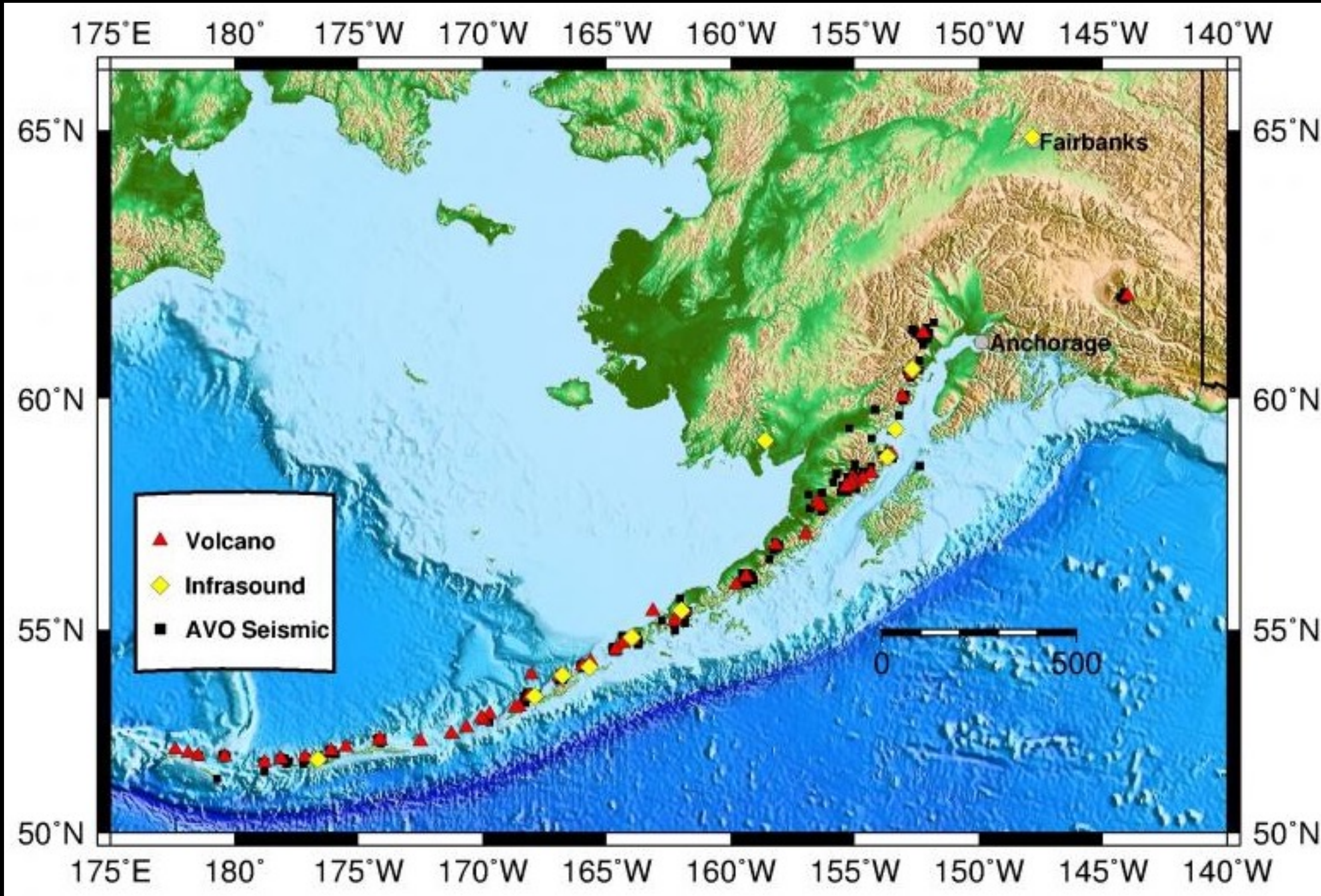

> 50 Historically Active (since 1760)

~ 90 active in last 10,000 years

> 130 volcanoes and volcanic fields active within the last 2 million years

Primary Hazard:

Aviation

EarthScope Transportable Array

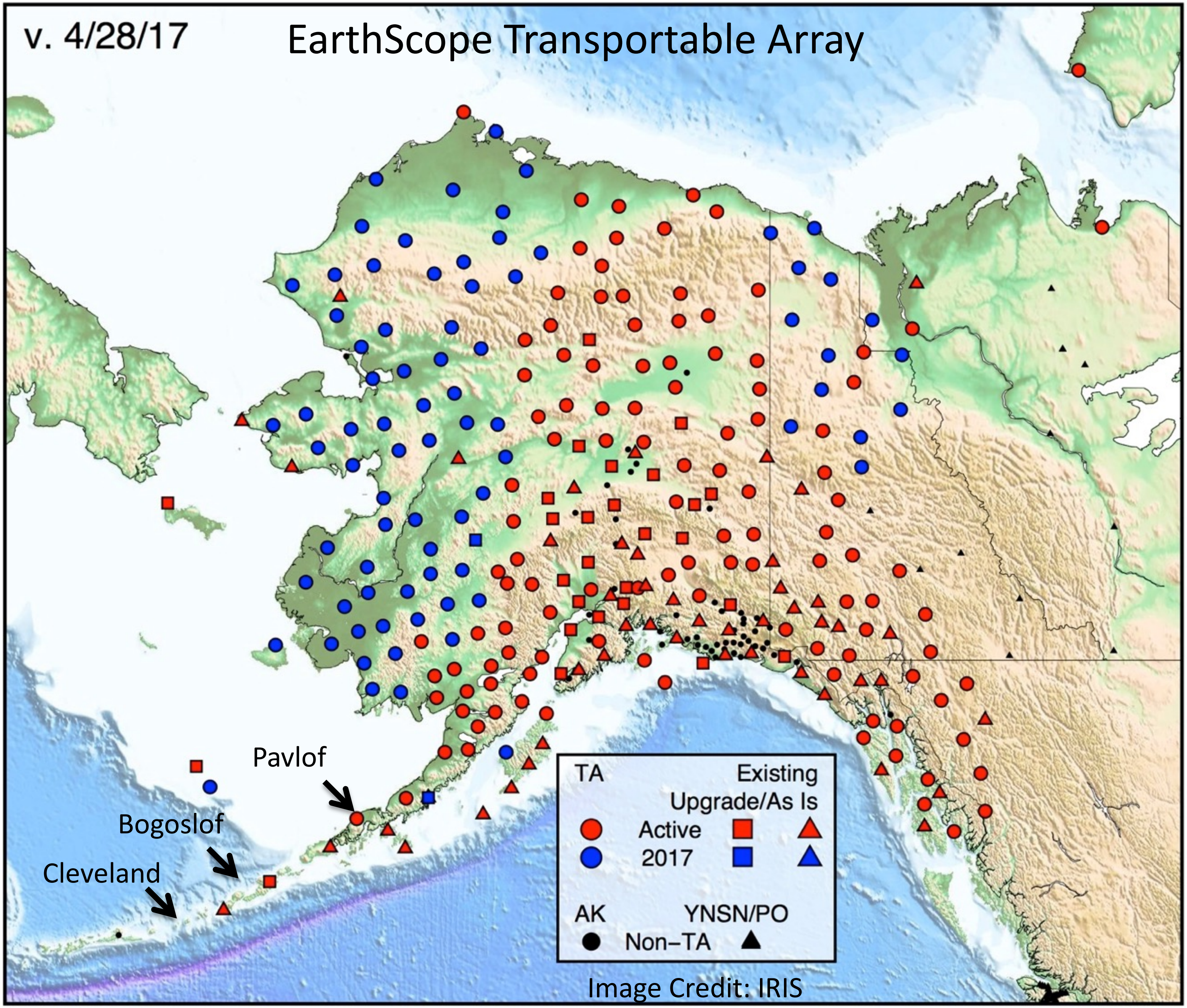

Image Credit: IRIS

The TA Stations Have Infrasound Sensors

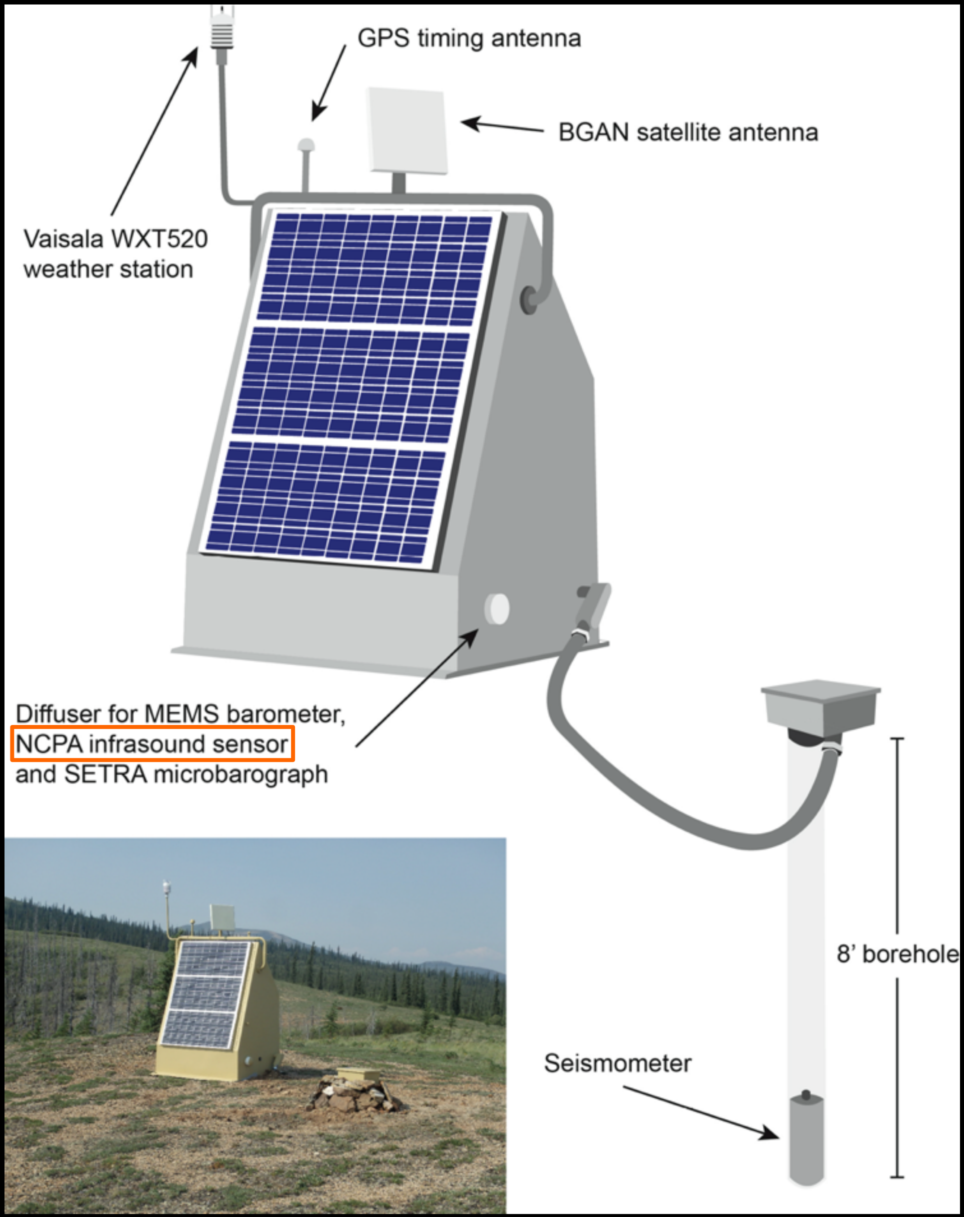

Most data transmitted in real-time

Image Credit: IRIS

Volcano Infrasound

- Most volcanic acoustic energy is emitted in the infrasound band (0.1-20 Hz)
  - Below the threshold of human hearing
- Not affected by cloud cover and can travel long distances
  - Low attenuation
- Can be used to detect, locate, characterize, and quantify volcanic eruptions

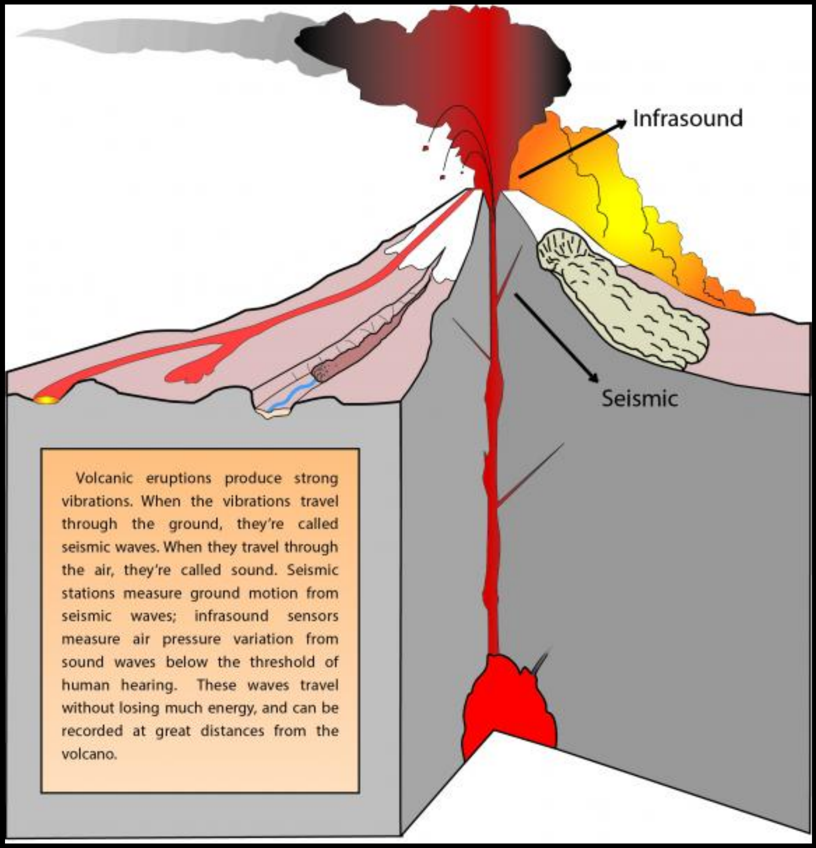

Image Credit: AVO

Refraction of Infrasound in the Atmosphere

- Static Sound Speed:

$$c = \sqrt{\gamma R T}$$

- Effective Sound Speed:

$$c_{eff} = c + \boxed{\vec{v} \cdot \vec{n}}$$

Wind component in the direction of propagation

- Snell's Law:

$$\frac{\sin\theta_1}{\sin\theta_2} = \frac{v_1}{v_2}$$

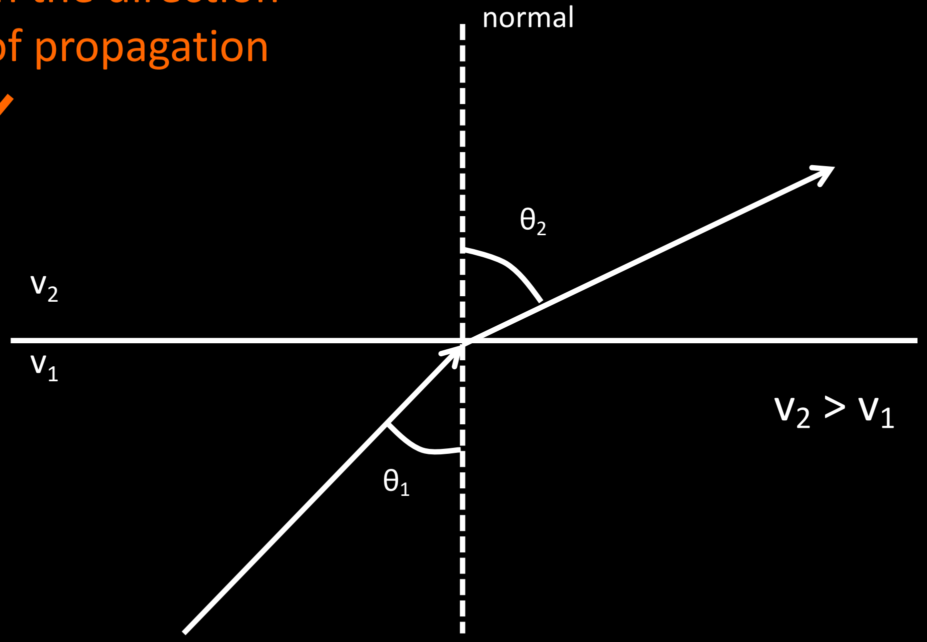

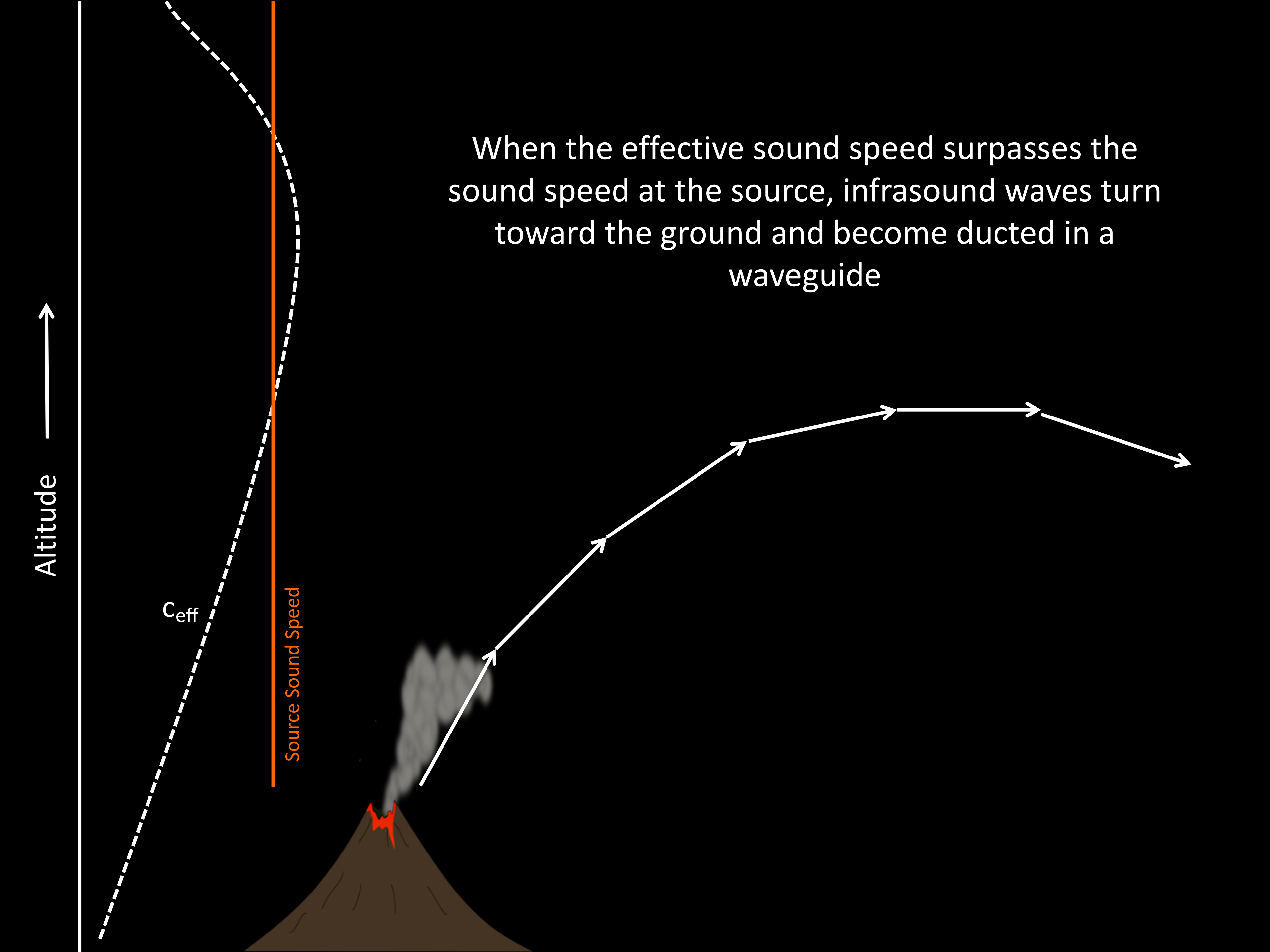
When the effective sound speed surpasses the sound speed at the source, infrasound waves turn toward the ground and become ducted in a waveguide
Altitude
c_{eff}
Source Sound Speed

Atmospheric Structure and Waveguides

Thermospheric Waveguide (0 to ~120 km):

- Signals are much fainter

Stratospheric Waveguide (0 to ~50 km):

- Dependent on wind jets that reverse with the season
  - East in the winter hemisphere
  - West in the summer hemisphere

Tropospheric Waveguide (0 to ~20 km):

- Arrive at a station the fastest with highest amplitude
- Dependent on day-to-day weather conditions
- Waveguides can disappear over long distances

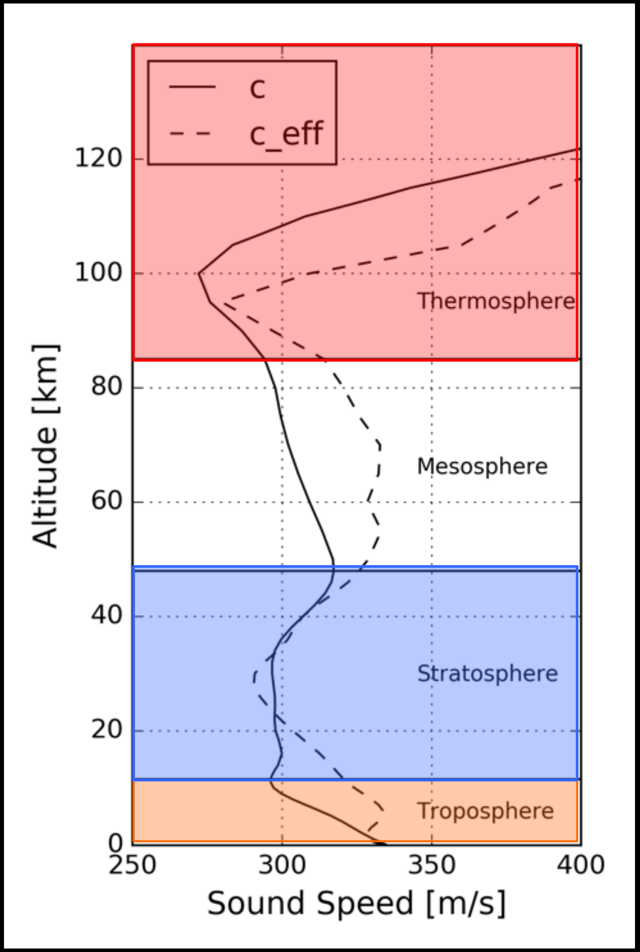

Wind Velocity Differences as a Function of Altitude

Uses NRLG2S model (Drob et al., 2003)

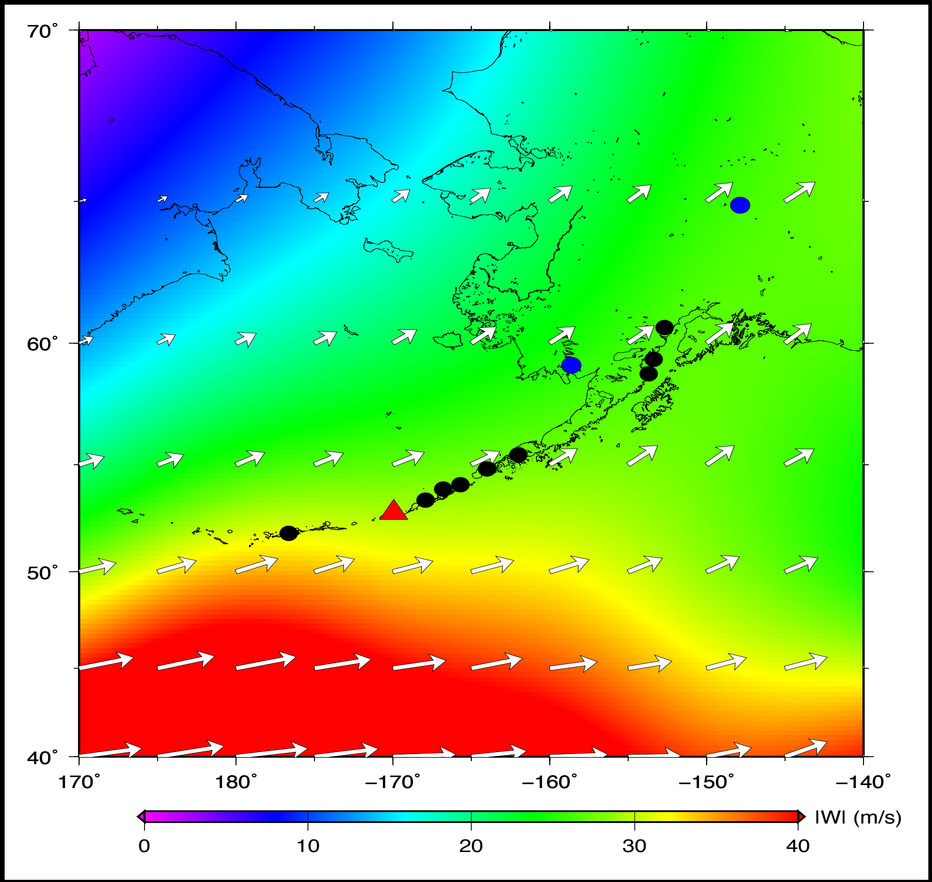

15 km altitude
(troposphere)

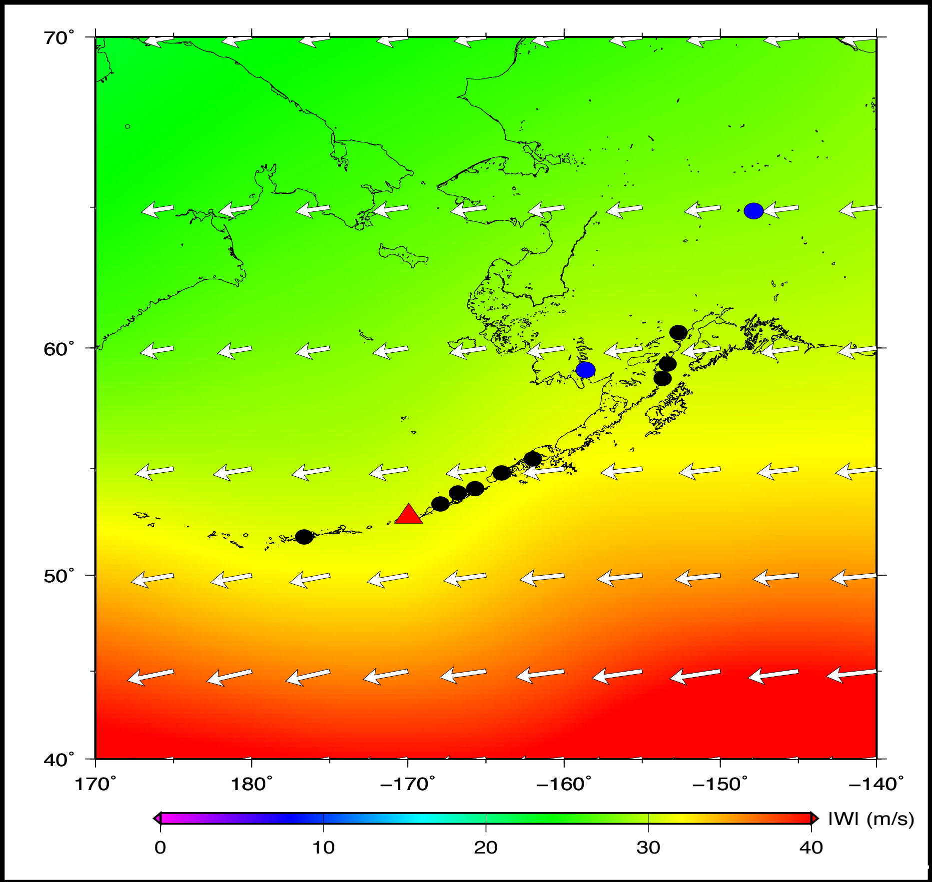

50 km altitude winds
(stratosphere)

A New Model to Constrain Atmospheric Conditions AVO-G2S

- We only have high resolution (temporally and spatially) atmospheric specifications for the lower atmosphere (~35 km), but infrasound can be guided to ~120 km
- Use atmospheric specifications for the lower atmosphere to extrapolate for the upper atmosphere, creating a seamless reconstruction of the atmospheric parameters
- Atmospheric models can be reconstructed at an arbitrary resolution and sub-sampled on 1-D columns, 2-D transects, or 3-D volumes for use with the GeoAc ray tracing software (Blom, 2014)

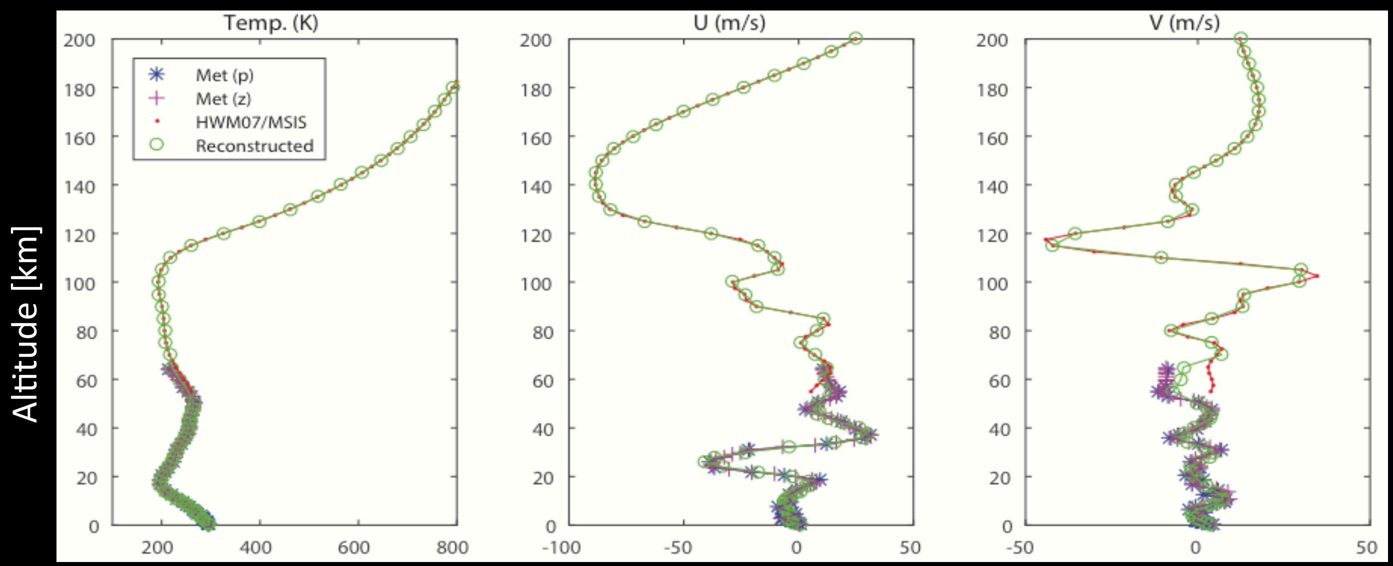

Sample reconstruction of atmospheric conditions using the new model:

Blue: raw pressure levels.

Magenta: raw data after interpolation plotted in altitude.

Green: reconstructed model.

Red: empirical data for upper atmosphere

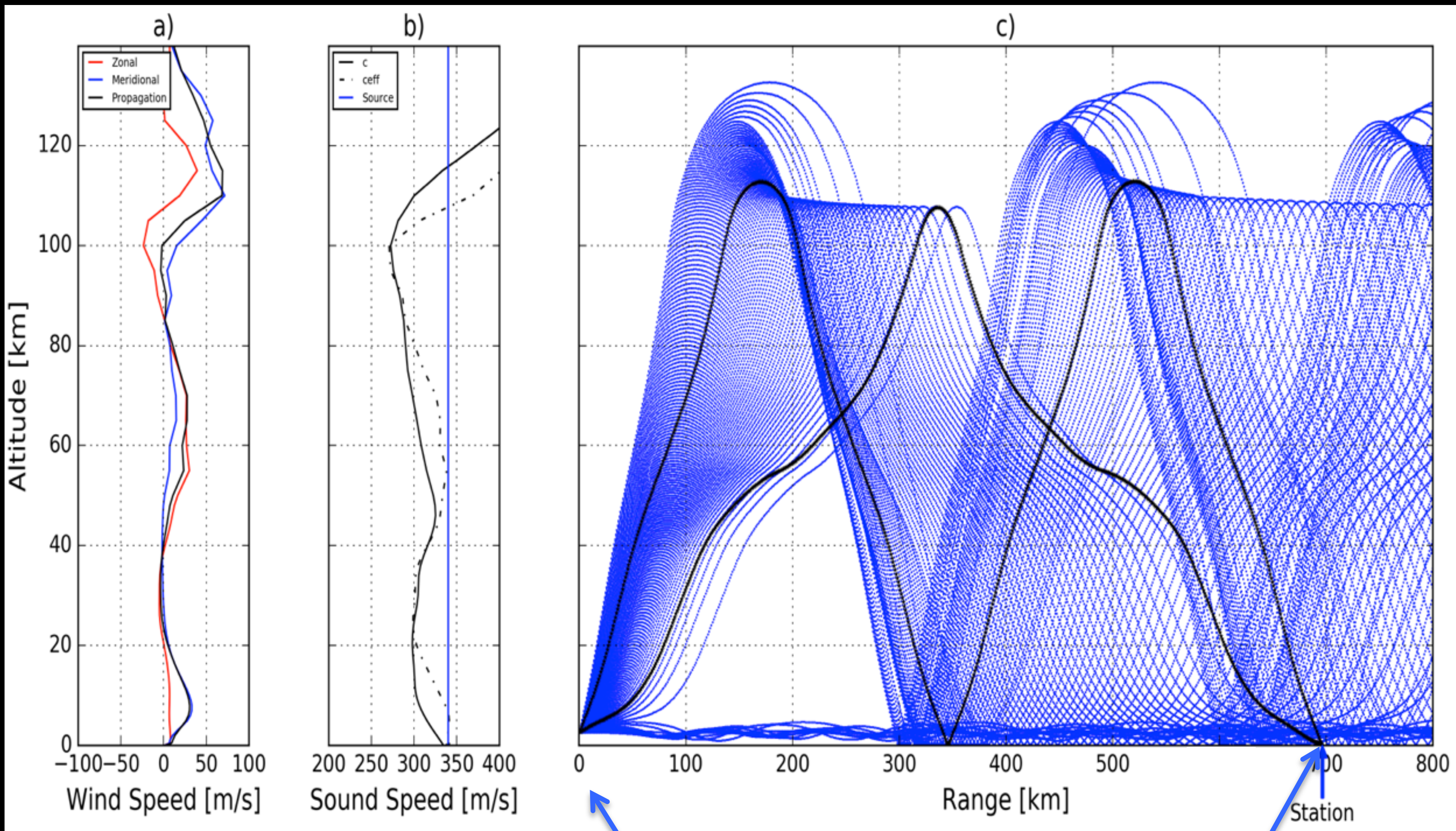

Red: Zonal (West to East)

Blue: Meridional (South to North)

Direction of Propagation

Solid Line: Sound Speed

Dotted Line: Effective Sound Speed

Vertical: Source Sound Speed

Ray tracing: visualization of the likely propagation path acoustic waves will travel

Eigen-rays: ray that connects source and receiver directly

- Traveltime

Cleveland Volcano

Photo Credit: John Lyons, AVO-USGS

- One of the most active volcanoes in the Aleutians
- ~~44~~ 45 explosions since 25 December 2011
  - Most recent: ~~24 March 2017~~ Last Night!
- Little to no precursory activity before explosions
- First local instrumentation installed in Summer 2014
  - Prior: Closest seismic station was 75 km east
  - Remote sensing was heavily relied upon

Cleveland Volcano: Difference in Detection at Long-Range

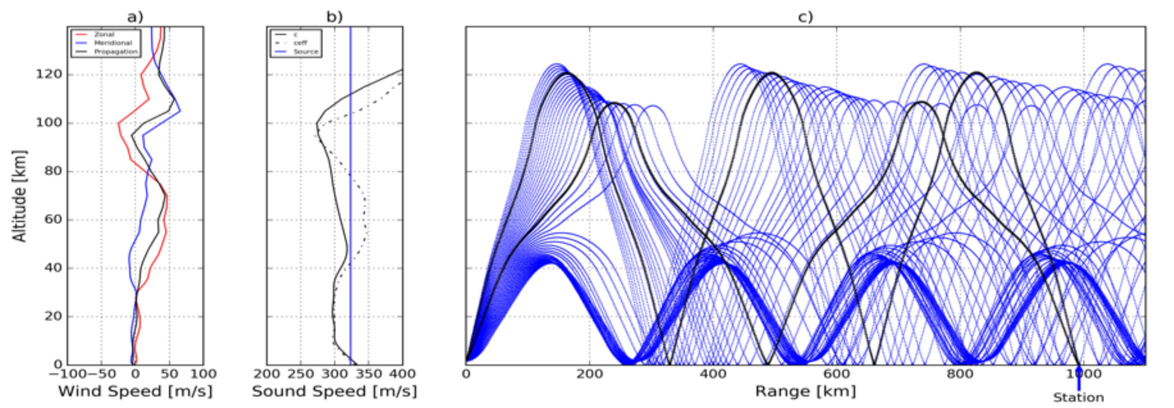

06-November-2014 (07:42 UTC)

*** Signal NOT detected in real time ***

Moderately strong stratospheric duct

No tropospheric duct predicted

No direct arrival at station, though energy is likely to be diffracted at long distances

21-July-2015 (16:17 UTC)

*** Explosion detected in real-time ***

Tropospheric Winds blowing to northeast at ~40 m/s

Strong low altitude (<10 km) tropospheric duct with numerous eigenrays

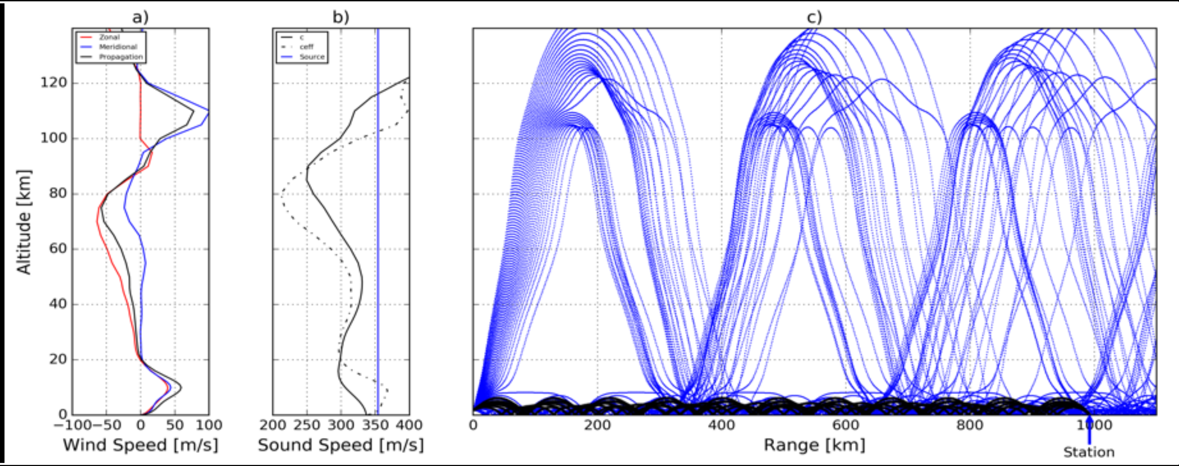



Pavlof Volcano

- Ashfall hazard for local communities
  - E.g. Nelson Lagoon, Sand Point, Cold Bay, King Cove
- Low-energy lava fountaining, lahars, and emissions of ash, gas and steam
- Very little precursory activity
  - ~ 20 minutes of low-level seismic tremor before recent eruption (March 2016)
- Affects air travel for days
  - March 2016: Cancelled over 100 flights

Pavlof Volcano: November 2014

- Eruption Onset: ~00:00 UTC on 13-Nov-2014
- … and remote sensing
- … nd become strong ~24 hours … UTC on 14-Nov-2014

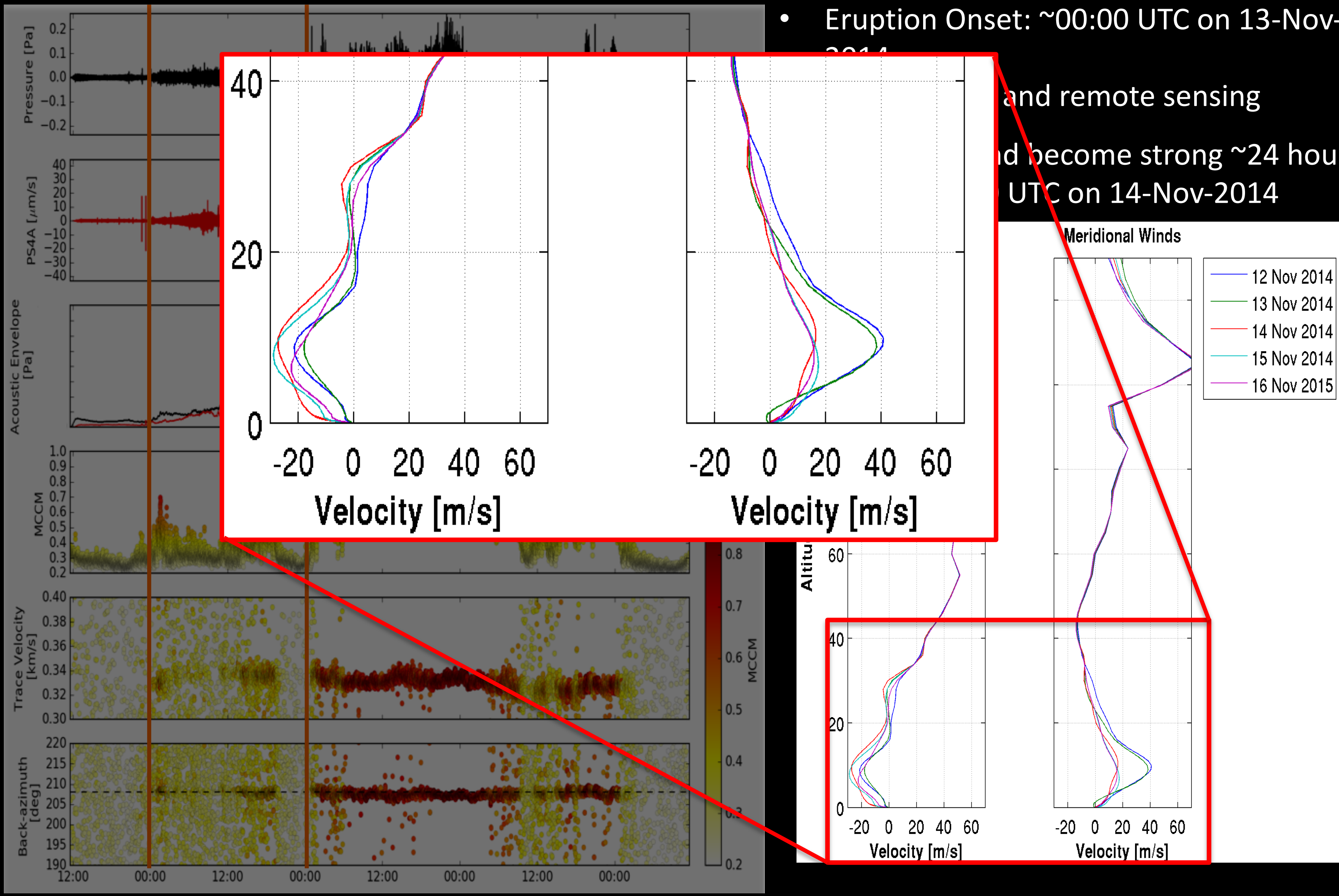

Pavlof Volcano: March 2016
First Known Volcanic Eruption Detected by TA

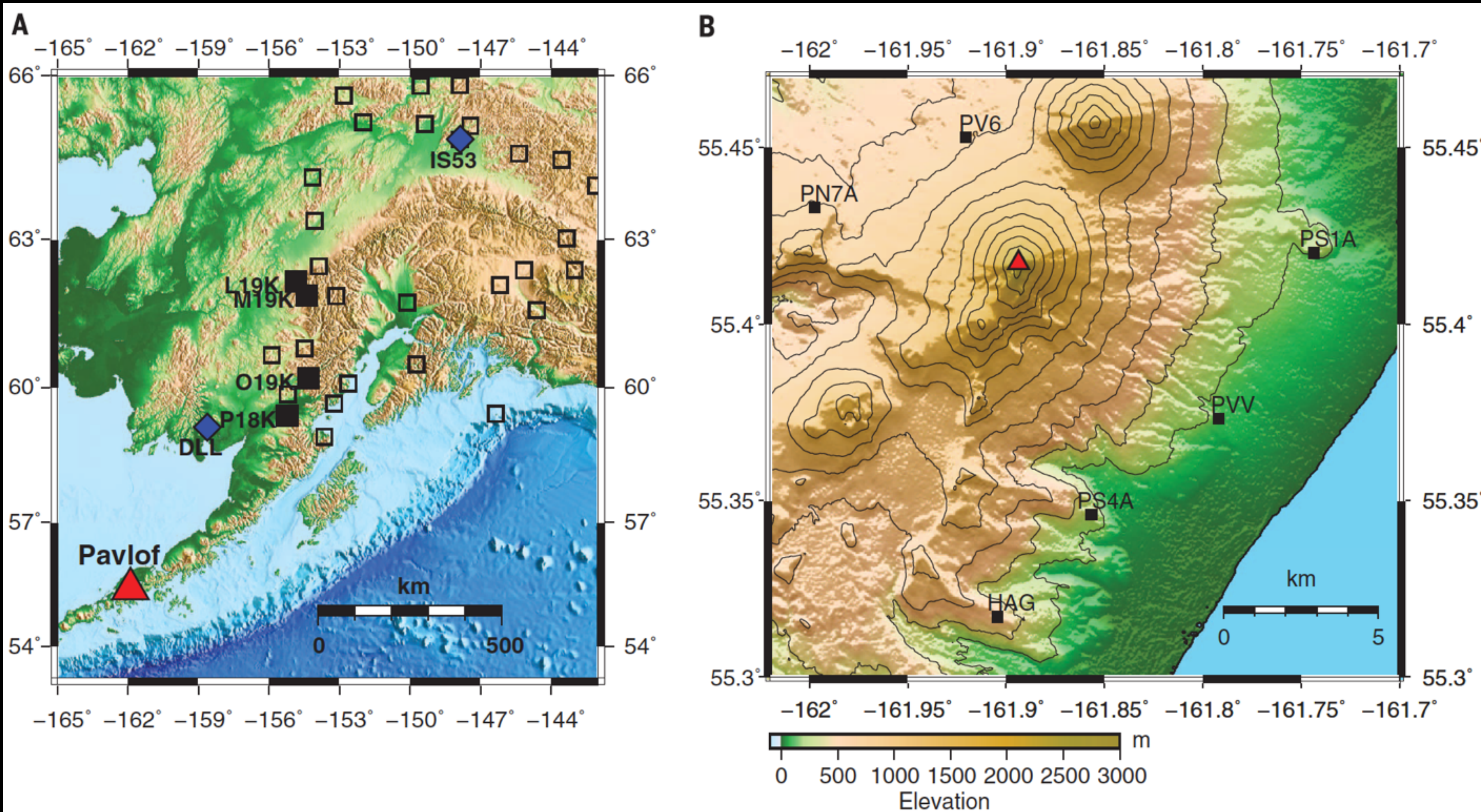

Fee et al., *Science*, 2017

Pavlof Volcano: March 2016

- Likely tropospheric arrivals
- Very little change in winds throughout the erution

  ➡Long-range infrasound reflects changes in source

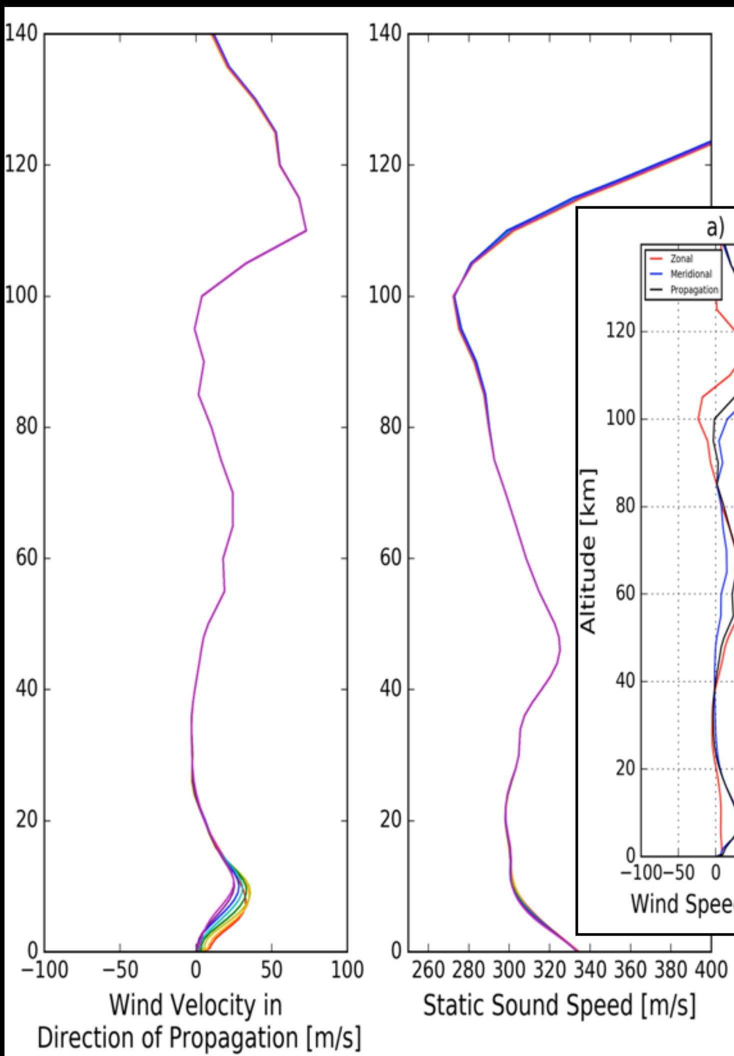

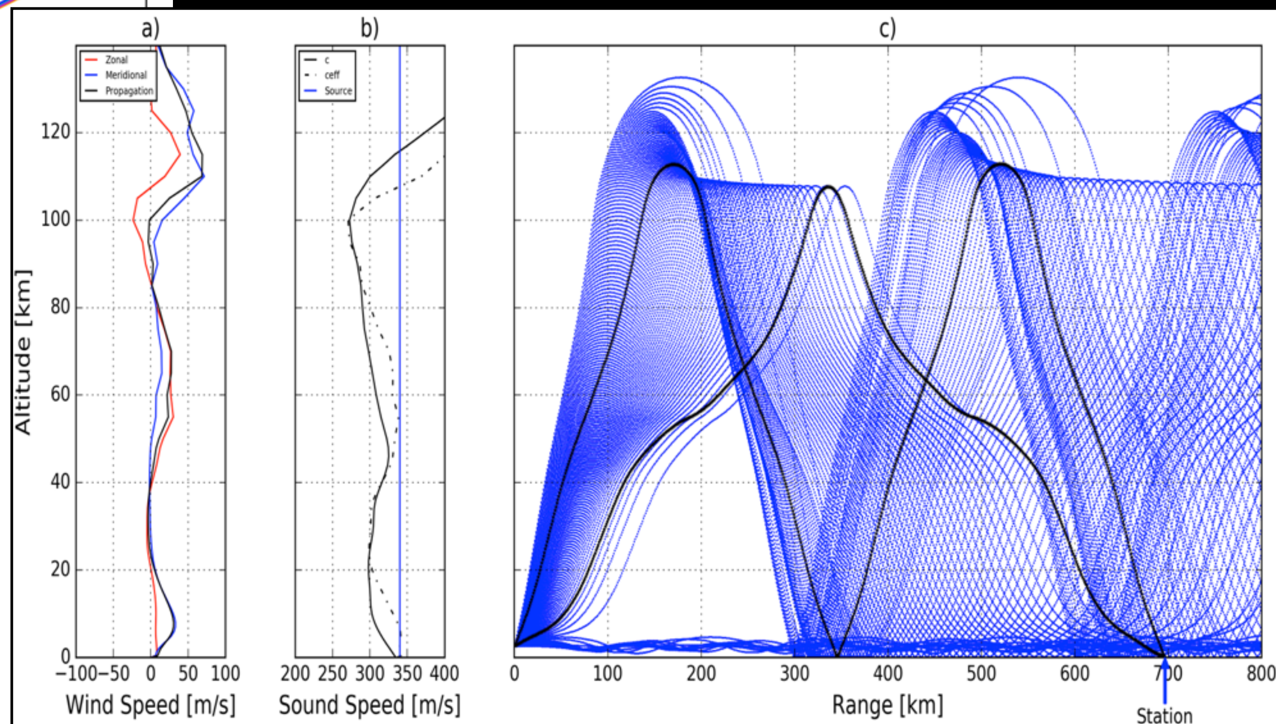

Bogoslof Volcano

- Eruption began on December 12, 2016
- Volcanic clouds to altitudes of 20,000 to 35,000 ft asl
- Trace ash fall in Unalaska/Dutch Harbor on January 31, 2017
- No ground-based monitoring equipment
  - Nearest seismic station ~50 km away
  - Long-range infrasound and lightning were key in detecting explosions

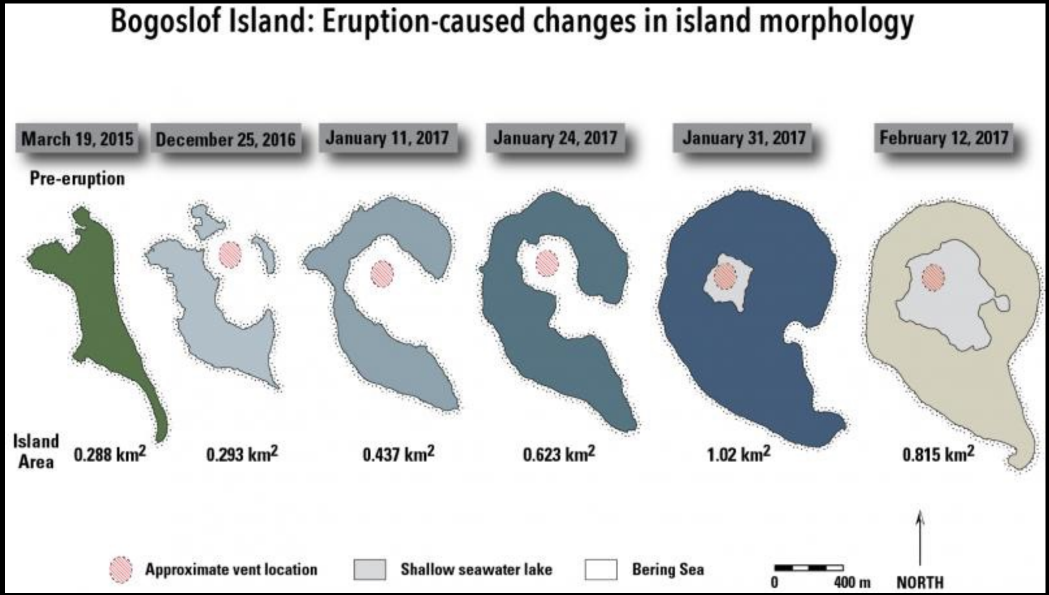

Image Credit: Chris Waythomas, USGS/AVO

Bogoslof Volcano 2016: Record Section of TA Stations

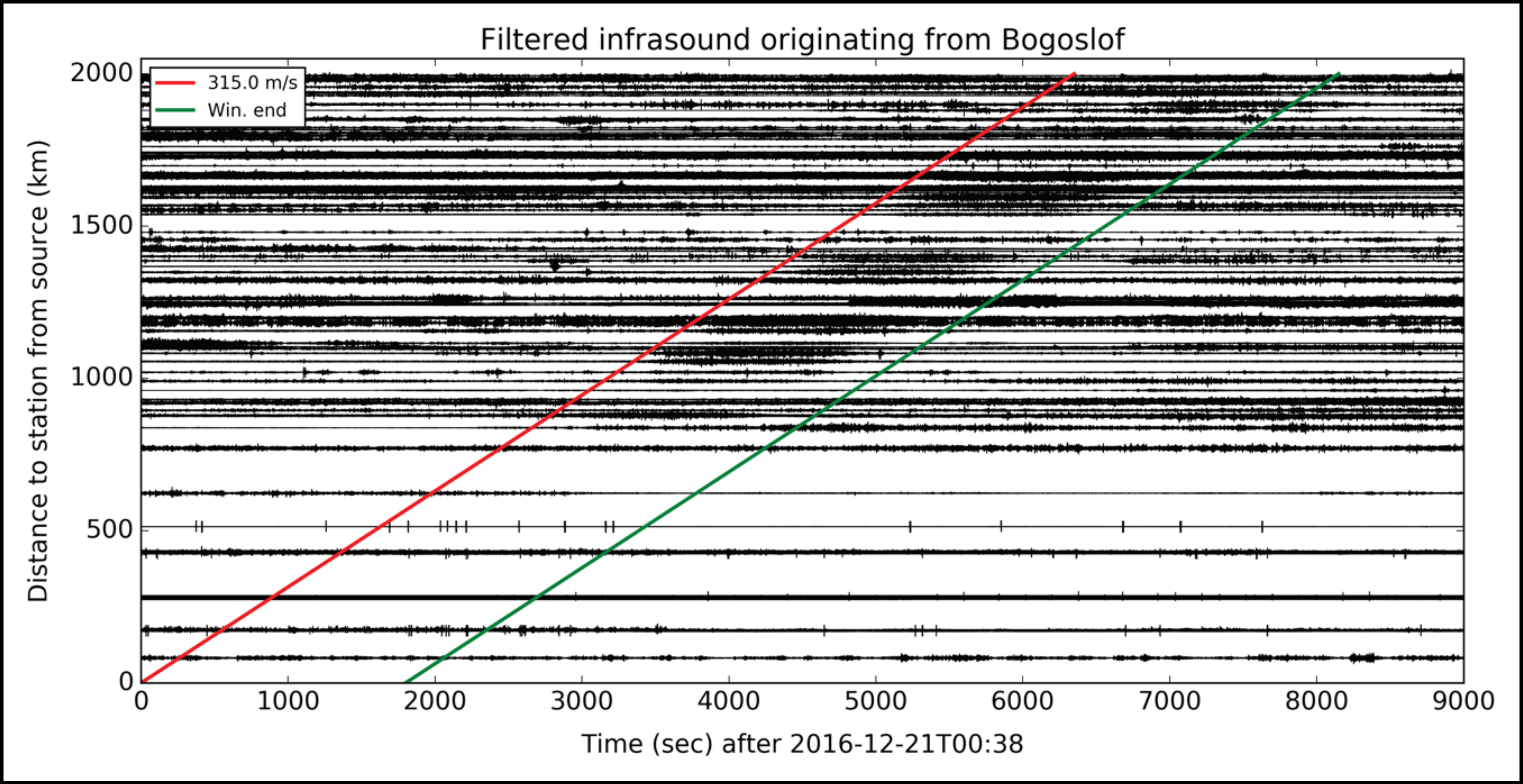

*** Most TA infrasound stations are seeing the eruption signal ***

Sanderson et al.
(Poster #23)

Bogoslof Event Location

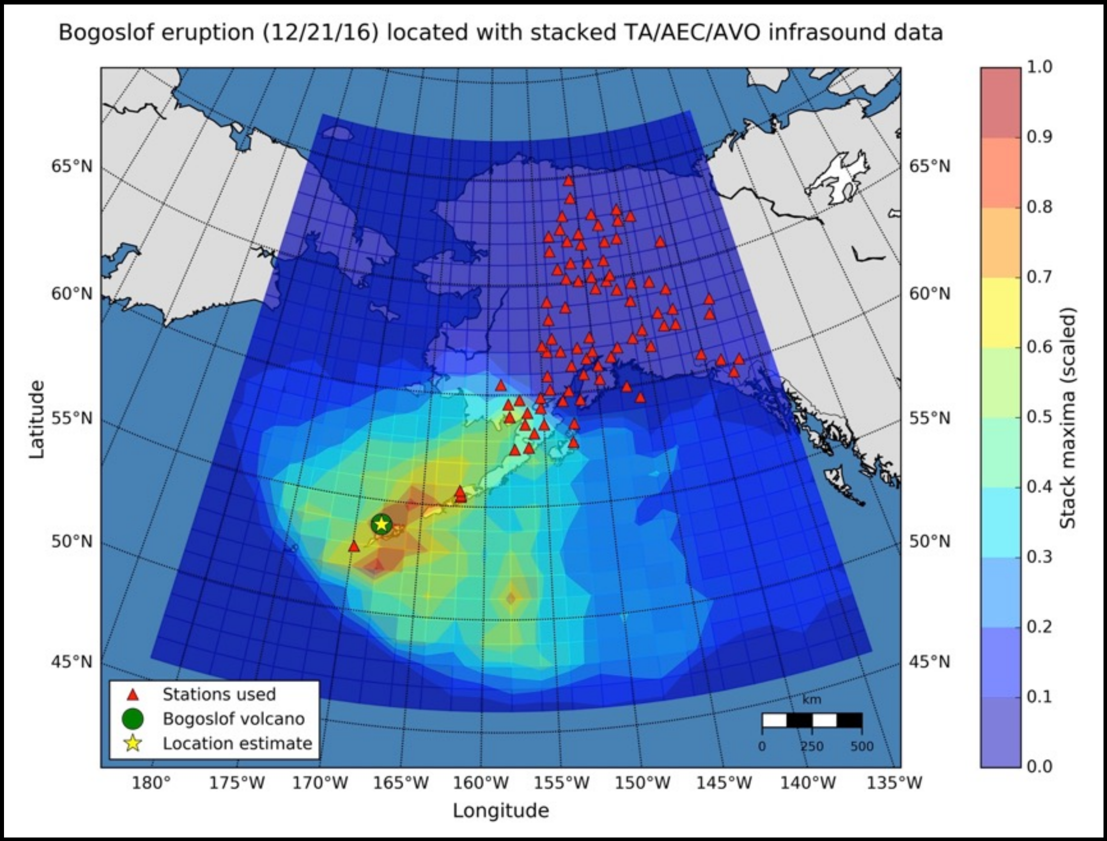

Sanderson et al.
(Poster #23)

- **Reverse Time Migration Algorithm**
  - Grid search for source location
  - Uses single propagation speed for all stations and times
- **AVO-G2S:**
  - Unique propagation speed based on the changing atmospheric structure for each station/source pair
  - Improve source localization capabilities

Conclusions and Future Work

- Long-range infrasound signals are highly influenced by the propagation path
  - Atmospheric reconstruction models are necessary
  - Determine contribution of propagation effects to the signal detected

- The TA can be used to monitor volcanic eruptions in Alaska
  - Our model (AVO-G2S) will help understand signals seen on TA infrasound stations

- We are working towards real-time long-range infrasound propagation modeling in Alaska using AVO-G2S
  - Used in near real-time for Pavlof 2016 and Bogoslof 2016-2017


Thank you

References

- Blom, P. S. (2014). GeoAc: Numerical tools to model acoustic propagation in the geometric limit [Computer Software]. Los Alamos National Laboratory
- Drob, D.P., Picone, J. M., and Garcés, M. (2003). Global morphology of infrasound propagation. *Journal of Geophysical Research: Atmospheres (1984–2012)*108(D21).
- Fee, D., Haney, M.M., Matoza, R.S., van Eaton, A.R., Cervelli, P., Schneider, D.J., and Iezzi, A.M. (2017). Volcanic tremor and plume height hysteresis from Pavlof Volcano, Alaska. *Science, 355(6320)*, 45-48.

A New Model to Constrain Atmospheric Conditions

- We follow the method outlined by Drob et al., (2003) for the Naval Research Lab Ground-To-Space (G2S) model

1. Extend a global grid of lower-atmospheric values to the upper- atmosphere
2. Populate the upper-atmospheric nodes with values derived from the empirical models
3. Decompose each dataset into their spherical harmonic coefficients
4. Generate a smooth representation of the spherical harmonic coefficients as a function of height. As suggested in Drob et al., (2003), we use the B-Spline representation. From this set of coefficients, spherical harmonic coefficients can be retrieved for any altitude; then the values of interest (meridional and zonal winds, temperature) can be reconstructed

- In contrast to the NRL-G2S model, we perform scalar spherical harmonic decompositions of the individual velocity components rather than a vector spherical harmonic decomposition. Additionally, we perform all decompositions on altitude levels rather than pressure levels

Model Validation: Cleveland 29 Dec 2011

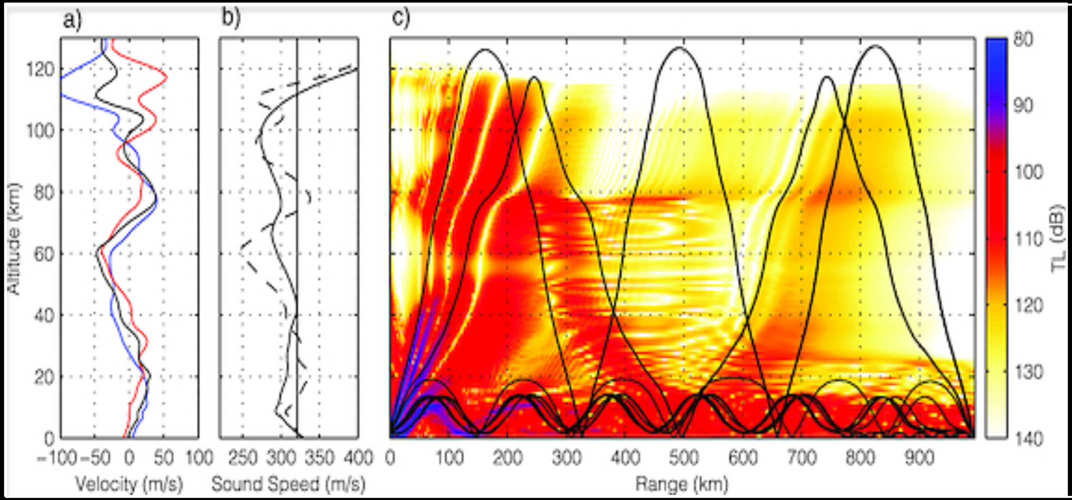

NRL-G2S (Drob et al., 2003):

From DeAngelis et al (2012)

Rays were primarily guided in troposphere and thermosphere

AVO-G2S:

Similar results

Predicted travel time for tropospheric duct are consistent with NRL-G2S at ~3139-3203 s

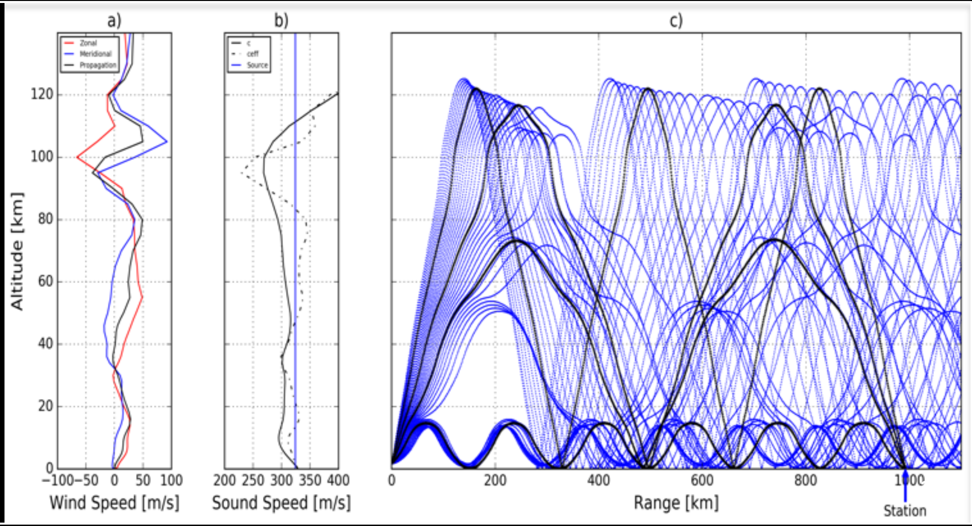

Cleveland Volcano

2014		2015
~0.6	**MCCM**	>0.8
0.329	**$C_{eff,rec}$ [km/s]**	0.339

06-November-2014

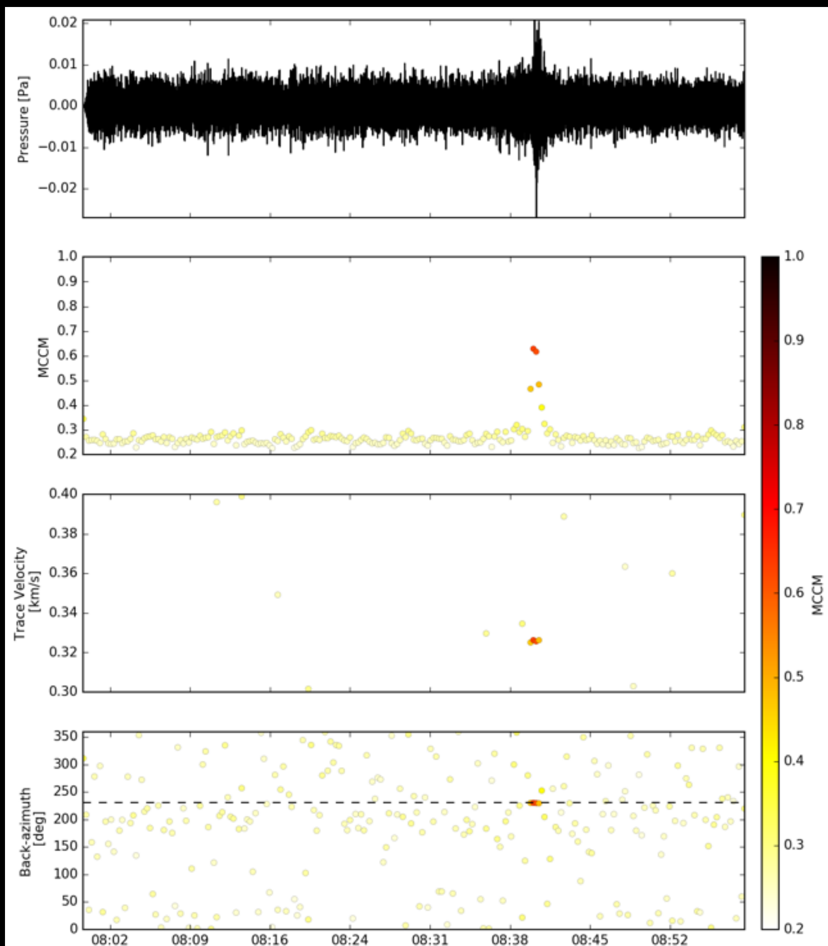

21-July-2015

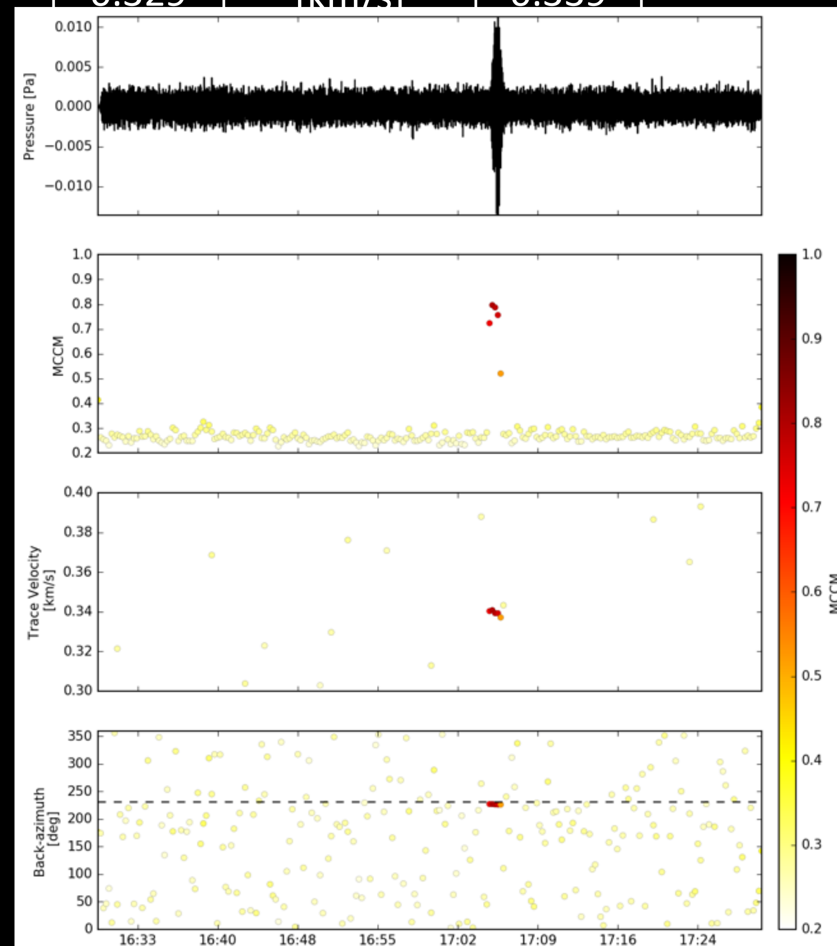

DLL data band passed between 1-5 Hz, beamformed, and time-corrected

Cleveland Volcano

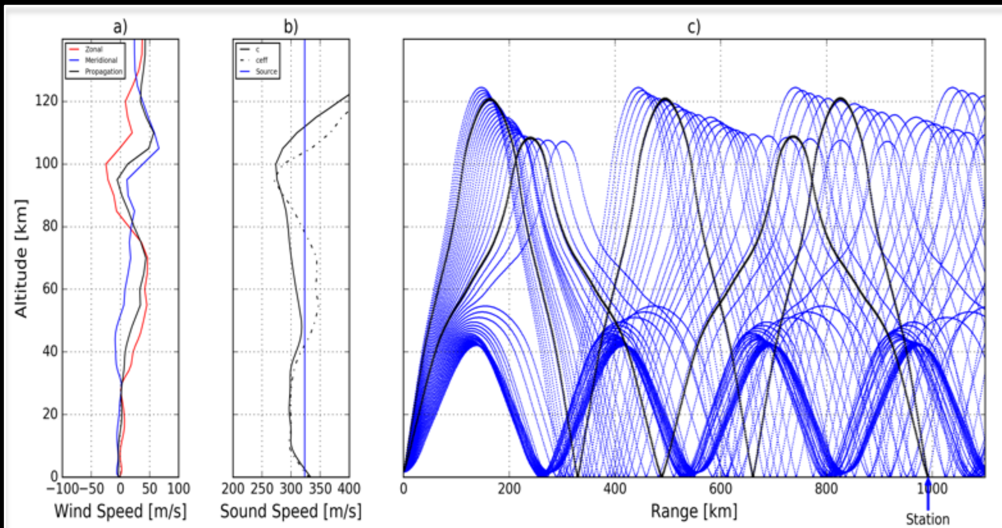

06-November-2014 (07:42 UTC)

Moderately strong stratospheric duct

No tropospheric predicted

DLL in "shadow zone"

21-July-2015 (16:17 UTC)

High Zonal and Meridional Winds ~40 m/s to the northeast

Very strong low altitude (<10 km) tropospheric duct with numerous eigenrays

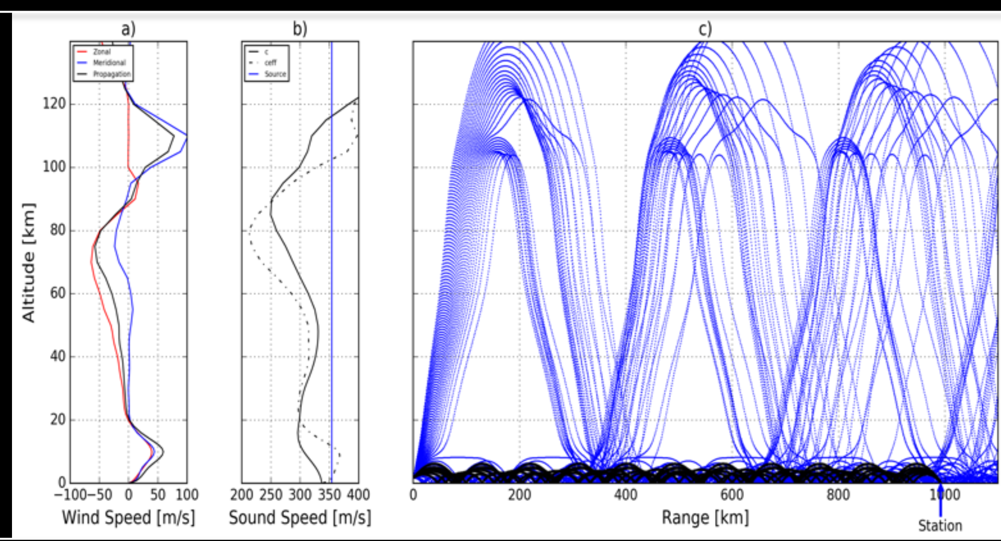

Pavlof Volcano

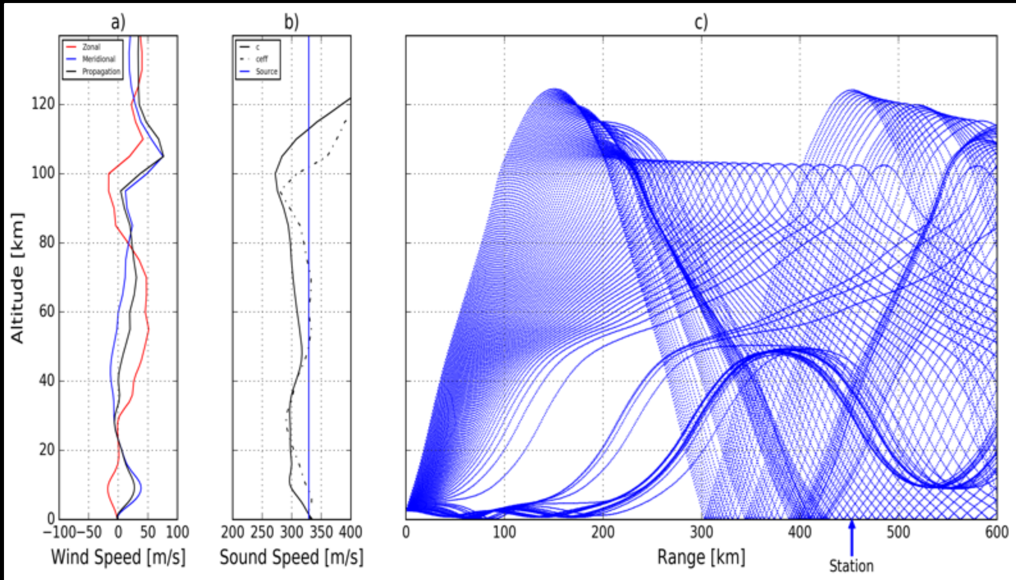

Nov-13-2014 at 00:00 UTC

Nov-14-2014 at 00:00 UTC

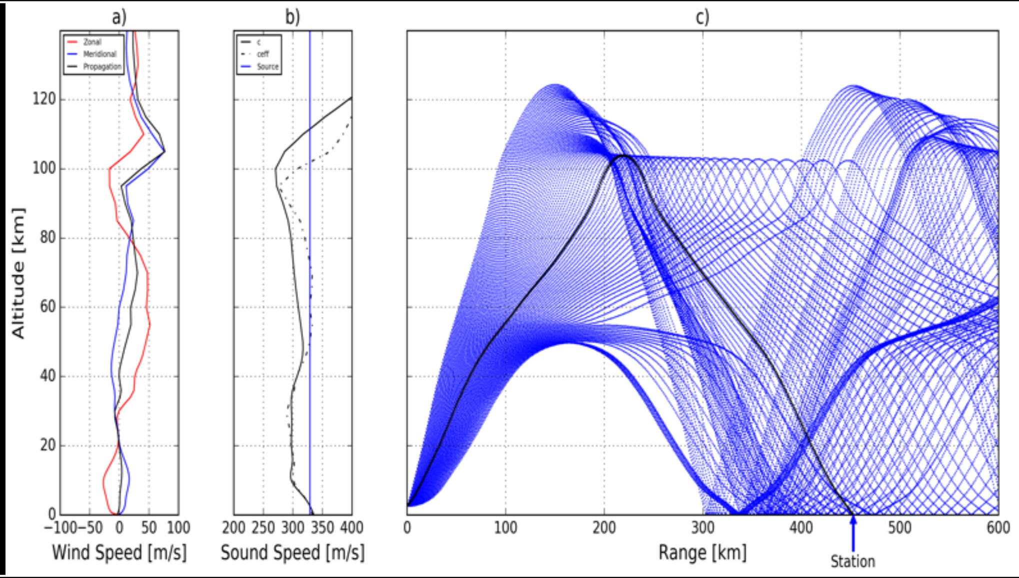

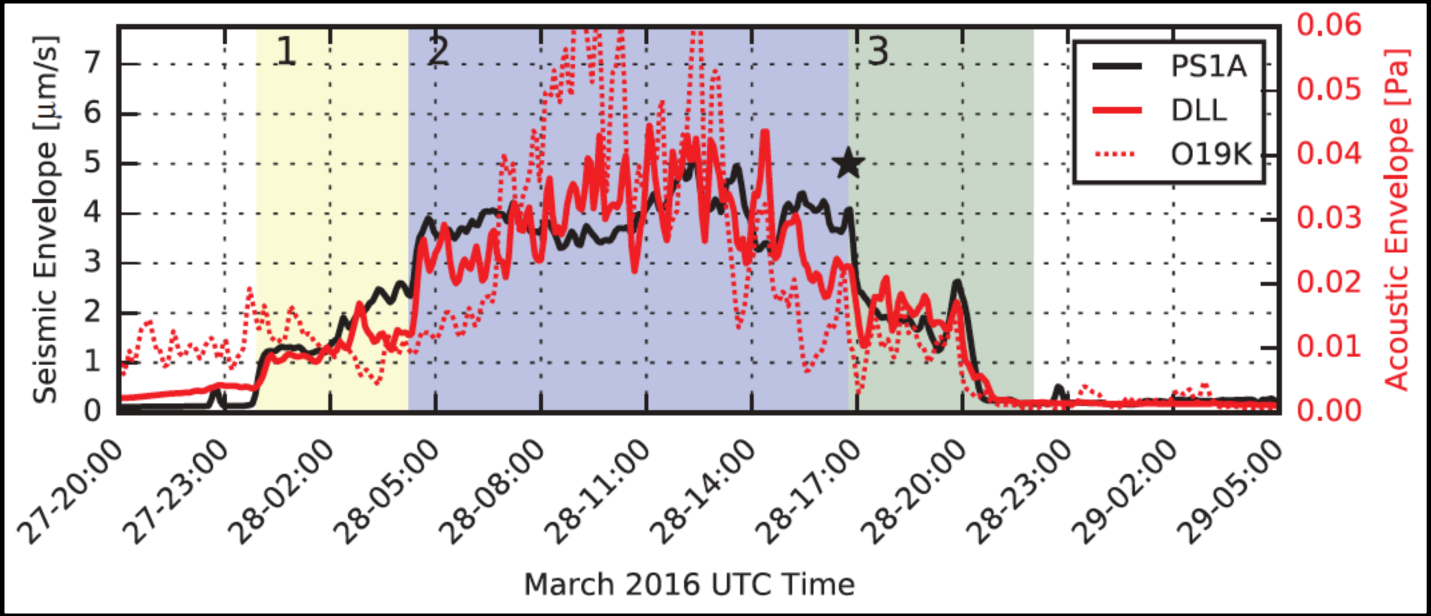

Fee et al., *Science*, 2017